Supporting Information

for

Unraveling the Role of the Protein Environment for [FeFe]-Hydrogenase: A New Application of Coarse-Graining

Martin McCullagh and Gregory A. Voth

Department of Chemistry, James Franck Institute, Institute for Biophysical Dynamics, and Computation Institute, The University of Chicago, Chicago, Illinois 60637. Phone: 773-702-9092. Fax: 773-795-9106. E-mail: gavoth@uchicago.edu.

FeS Molecular Dynamics Parameters

Initially, all the parameters for the nonstandard residues in [FeFe]-hydrogenase were taken from the paper by Chang et al.[1] It was found, however, that the FeS cuboids were not stable for trajectories longer than ~6 ns. The main issue was the internal stability of the iron-sulfur cuboids. A new topology and set of dihedral and angle parameters were defined to address this. For sake of clarity, all angle and dihedral parameters needed to define the FeS cuboids are included here even if they are taken directly from the work of Chang et al.[1] The atom types and topology of the FeS cuboid with four ligated cysteines are shown in Figure 1 and the parameters are listed in Tables 1-4. The atom types and topology of the FeS cuboid with three ligated cysteines and one ligated histidine are shown in Figure 2 and the parameters are listed in Tables 5-8.

Marcus Electron Transfer Rates

The standard form of the Marcus electron transfer rate is:

$$k_{ET} = H_{AB}^2 \sqrt{\frac{4\pi^3}{h^2 \cdot \lambda \cdot k_B T}} \cdot exp\left[\frac{-\Delta F^\dagger}{k_B T}\right] \qquad \text{(SI 1)}$$

Where λ is the total reorganization energy, $\Delta F^\dagger$ is the barrier height, and H_{AB} is the electronic coupling term. For our crude approximation we assume $\lambda \approx \lambda_{outersphere}$ and $H_{AB} = 0.1\ cm^{-1}$ for all steps. Given these assumptions, the ET rates for the three steps can be calculated from the reorganization energies and barrier heights given in the main text. The electron transfer rates for the three forward reactions are 4.7 s^{-1}, 2300 s^{-1} and 4400 s^{-1}. The reverse reactions have an additional barrier height due to the negative free energy differences and are calculated as $1.3 \times 10^{-8}\ s^{-1}$, $3.3 \times 10^{-8}\ s^{-1}$ and $1.3 \times 10^{-9}\ s^{-1}$. In order to determine the overall

rate of electron transfer from cluster D to the active site we must come up with a kinetic model. Consider the following scheme:

$$D^{2-} \underset{k_{-1}}{\overset{k_1}{\leftrightarrows}} C^{2-} \underset{k_{-2}}{\overset{k_2}{\leftrightarrows}} B^{2-} \underset{k_{-3}}{\overset{k_3}{\leftrightarrows}} H^{2-}$$

Given that the reverse reactions are at least eight orders of magnitude slower than the forward reactions, we can compute the overall rate simply as the reciprocal sum of the forward rates:

$$\frac{1}{k_{total}} = \frac{1}{k_1} + \frac{1}{k_2} + \frac{1}{k_3} \qquad \text{(SI 2)}$$

This yields a value of 4.7 s^{-1} for the overall rate of electron transfer from the outer 4FE4S center to the active site.

Electrostatic Potential of CG sites at Active Site

In addition to the electron transport pathway the electrostatic potential (ESP) at the active site plays an important role in catalysis.[2] It has been known for some time that the amino acid neighborhood around an active site plays an important role in stabilizing the compound as well as potential transition states during the catalytic process.[2,3] It has been shown recently that mutation to residues around the [FeFe]-hydrogenase active site can lead to reduced catalytic activity and possibly to a complete destabilization of the active site structure.[4] Specifically, mutations of residues MET353, LYS358, and MET497 (all shown in Figure 1(b)) lead to little or no catalytic activity of [FeFe]-hydrogenase.[4] In order to determine which areas of the protein are contributing strong ESP to the active site we have computed the average ESP on a 5 Å x 5 Å x 5 Å grid centered at the center-of-mass of the active site with a 1 Å spacing. Similar to the electron transport parameters, the ESP was decomposed into CG sites and solvent contributions.

The decomposed ESP for the base H_{ox} state of [FeFe]-hydrogenase was computed. The resulting probability distribution of ESP values for CG sites 4-7 and the solvent are shown in Figure 10. CG sites 1 and 2 are not shown because they are too far away from the active site to have any effect. Similarly CG site 3 shows very little contribution to the overall ESP having a narrow distribution centered at -1.0 k_BT/e. CG sites 4 and 5 have a strong positive ESP at the active site stabilizing any negative charge that is present. CG site 6, on the other hand, has a strong negative ESP (centered at -17 k_BT/e) that stabilizes the positive charge at the active site. CG site 7 has a small but interesting contribution to the ESP, exhibiting a bimodal distribution centered around 2 k_BT/e. The bimodal nature of this distribution suggests that CG site 7 has two states in which it resides during the coarse of our simulation. The solvent also contributes to the ESP at the active site supplying a

broad distribution centered at 5 k_BT/e. The total contribution of the protein scaffold and the solvent averaged over the entire trajectory is 15.2 k_BT/e suggesting that a positive ESP may be important for stabilization of the active site and thus important for design of efficient biomimetic systems.

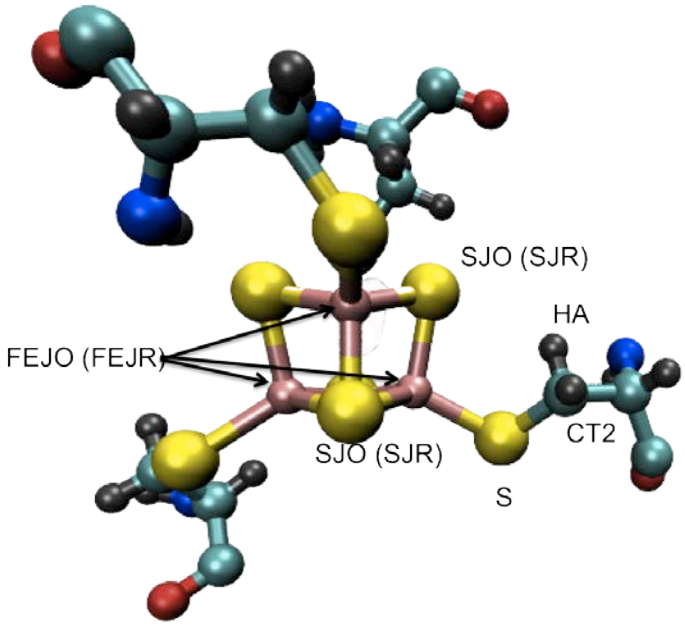

Figure 1 Depiction of a FeS cuboid in [FeFe]-hydrogenase with four ligated cysteines. The necessary atom types are given with the names of the reduced atom types in parenthesis where necessary.

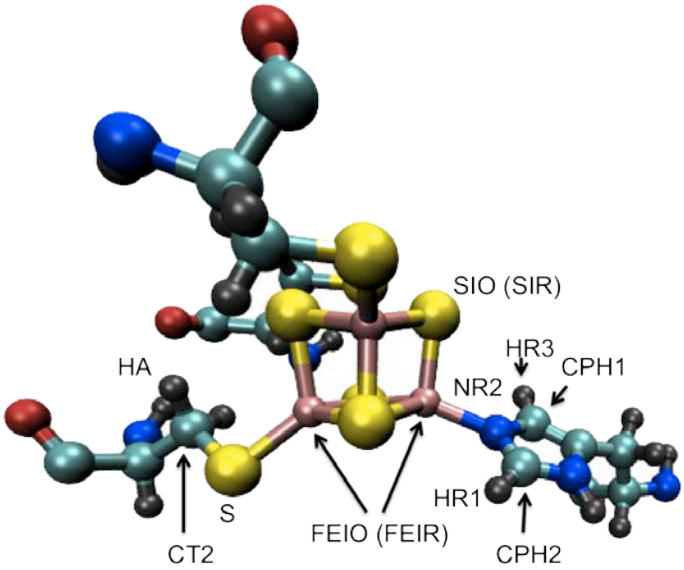

Figure 2 Depiction of the FeS cuboid in [FeFe]-hydrogenase with three ligated cysteines and a single ligated histidine. The important atom types are given with the reduced forms in parentheses where necessary.

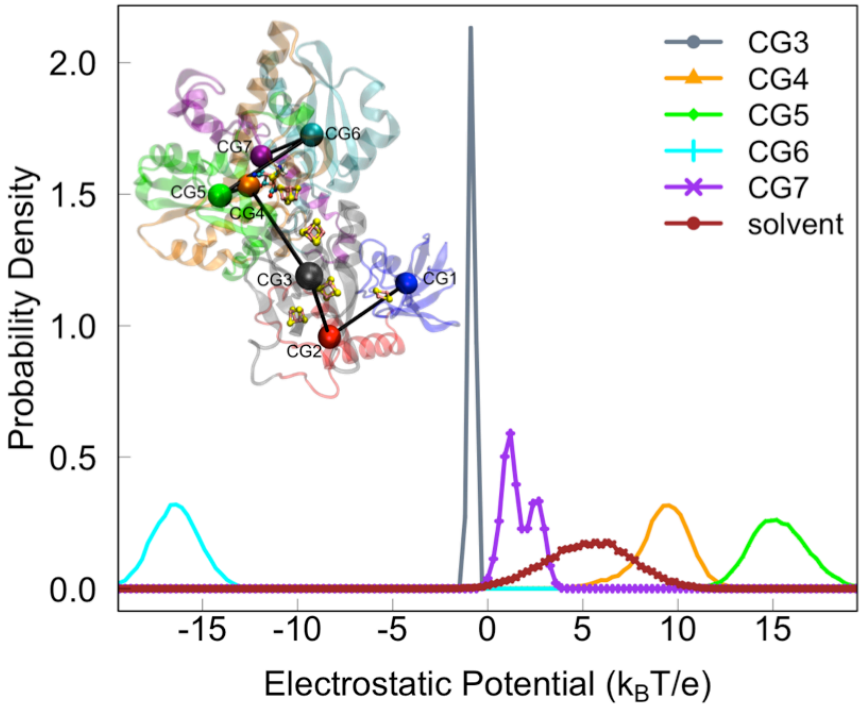

Figure 3. Probability density of the electrostatic potential at the active site of [FeFe]-hydrogenase computed in the fully oxidized form from a 50ns MD trajectory. The

reported ESP values represent an average value over a 5Åx5Åx5Å grid centered at the center-of-mass of the active site.

Table 1 Angle parameters for oxidized form of FeS cluster ligated to four cysteine residues.

Angle	k_θ (kcal/mol/rad^2)	θ_{eq} (degrees)
SJO-FEJO-SJO	4.313	103.69
FEJO-SJO-FEJO	2.725	74.35
S-FEJO-SJO	12.449	114.73
CT2-S-FEJO	74.621	106.29

Table 2 Angle parameters for reduced form of FeS cluster ligated to four cysteine residues.

Angle	k_θ (kcal/mol/rad^2)	θ_{eq} (degrees)
SJR-FEJR-SJR	2.034	105.11
FEJR-SJR-FEJR	1.299	72.25
S-FEJR-SJR	12.618	113.54
CT2-S-FEJR	72.292	105.32

Table 3 Dihedral parameters for oxidized form of FeS cluster ligated to four cysteine residues.

Dihedral	k_ϕ (kcal/mol)	n	δ (degrees)
FEJO-SJO-FEJO-SJO	8.00	4	180.0
S-FEJO-SJO-FEJO	10.64	6	0.0
FEJO-S-CT2-HA	14.03	3	0.0
FEJO-S-CT2-CT1	0.27	2	0.0
CT2-S-FEJO-SJO	1.17	6	0.0

Table 4 Dihedral parameters for the reduced form of an FeS cluster ligated to four cysteine residues.

Dihedral	k_ϕ (kcal/mol)	n	δ (degrees)
FEJR-SJR-FEJR-SJR	8.00	4	180.0
S-FEJR-SJR-FEJR	10.64	6	0.0
FEJR-S-CT2-HA	14.40	3	0.0
FEJR-S-CT2-CT1	0.27	2	0.0
CT2-S-FEJR-SJR	1.06	6	0.0

Table 5 Angle parameters for oxidized form of FeS cluster ligated to three cysteine residues and one histidine residue.

Angle	k_θ (kcal/mol/rad^2)	θ_{eq} (degrees)
SIO-FEIO-SIO	4.745	104.03
FEIO-SIO-FEIO	2.675	73.90
S-FEIO-SIO	12.723	114.51
CT2-S-FEIO	73.890	106.32
NR2-FEIO-SIO	2.675	114.08
CPH2-NR2-FEIO	35.997	127.85
CPH1-NR2-FEIO	35.074	126.25

Table 6 Angle parameters for reduced form of FeS cluster ligated to three cysteine residues and one histidine residue.

Angle	k_θ (kcal/mol/rad^2)	θ_{eq} (degrees)
SIR-FEIR-SIR	2.544	102.85
FEIR-SIR-FEIR	1.503	75.24
S-FEIR-SIR	2.544	102.85
CT2-S-FEIR	60.541	102.12
NR2-FEIR-SIR	61.550	110.00
CPH2-NR2-FEIR	26.185	133.63
CPH1-NR2-FEIR	29.651	119.56

Table 7 Dihedral parameters for oxidized form of FeS cluster ligated to three cysteine residues and one histidine.

Dihedral	k_ϕ (kcal/mol)	n	δ (degrees)
FEIO-SIO-FEIO-SIO	8.00	4	180.0
S-FEIO-SIO-FEIO	10.64	6	0.0
FEIO-S-CT2-HA	14.03	3	0.0
FEIO-S-CT2-CT1	0.27	2	0.0
CT2-S-FEIO-SIO	1.17	6	0.0
NR2-FEIO-SIO-FEIO	1.01	4	386.24
FEIO-NR2-CPH2-HR1	1.88	1	180.0
FEIO-NR2-CPH2-NR1	3.07	1	0.0
FEIO-NR2-CPH1-HR3	2.04	1	180.0
FEIO-NR2-CPH1-CPH1	3.12	1	0.0
SIO-FEIO-NR2-CPH1	1.93	3	0
SIO-FEIO-NR2-CPH2	1.92	3	180.0

Table 8 Dihedral parameters for the reduced form of an FeS cluster ligated to three cysteine residues and one histidine residue.

Dihedral	k_ϕ (kcal/mol)	n	δ (degrees)
FEIR-SIR-FEIR-SIR	8.00	4	180.0
S-FEIR-SIR-FEIR	10.64	6	0.0
FEIR-S-CT2-HA	14.03	3	0.0
FEIR-S-CT2-CT1	0.27	2	0.0
CT2-S-FEIR-SIR	1.17	6	0.0
NR2-FEIR-SIR-FEIR	6.60	4	386.24
FEIR-NR2-CPH2-HR1	2.64	1	180.0
FEIR-NR2-CPH2-NR1	3.79	1	0.0
FEIR-NR2-CPH1-HR3	2.12	1	180.0
FEIR-NR2-CPH1-CPH1	3.26	1	0.0
SIR-FEIR-NR2-CPH1	1.02	3	0
SIR-FEIR-NR2-CPH2	1.06	3	180.0

References

1. Chang, C. H. & Kim, K. Density Functional Theory Calculation of Bonding and Charge Parameters for Molecular Dynamics Studies on [FeFe] Hydrogenases. *J. Chem. Theory Comput.* **5**, 1137–1145 (2009).
2. Warshel, A., Sharma, P. K. & Kato, M. Electrostatic basis for enzyme catalysis. *Chem. Rev.* **106**, 3210–3235 (2006).
3. Loew, G. Role of the heme active site and protein environment in structure, spectra, and function of the cytochrome P450s. *Chem. Rev.* **100**, 407–419 (2000).
4. Knörzer, P. *et al.* Importance of the protein framework for catalytic activity of [FeFe]-hydrogenases. *J. Biol. Chem.* **287**, 1489–1499 (2012).